IV.H.4 An Integrated Approach of Hydrogen Storage in Complex Hydrides of Transitional Elements*

A. Bhattacharyya (Primary Contact), A.S. Biris, M.K. Mazumder, T. Karabacak, Ganesh Kannarpady, R. Sharma, M.F. Cansizoglu, H. Ishihara, M. Wolverton,[1] and D. Emanis

Department of Applied Science
University of Arkansas at Little Rock
2801 S. University Ave.
Little Rock, AR 72211
Phone: (501) 569-8007
E-mail: axbhattachar@ualr.edu
[1]Los Alamos National Laboratory

DOE Technology Development Manager: Ned Stetson
Phone: (202) 586-9995
E-mail: Ned.Stetson@ee.doe.gov

DOE Project Officer: Katie Randolph
Phone: (303) 275-4954
E-mail: Katie.Randolph@go.doe.gov

Contract Number: DE-FG36-06GO86054

Project Start Date: July 1, 2006
Project End Date: July 31, 2010

*Congressionally directed project

Objectives

- Investigation of maximum hydrogen storage capacity, adsorption/desorption kinetics, and catalyst effects in thin films and nanostructures of magnesium borohydride for hydrogen storage.
- Experimental investigation of methods to destabilize borohydrides in order to lower the temperature, and increase the rate of dehydrogenation/rehydrogenation.

Technical Barriers

This project addresses the following technical barriers from the Storage section of the Fuel Cell Technologies Program Multi-Year Research, Development and Demonstration Plan:

(P) Lack of Understanding of Hydrogen Physisorption and Chemisorption

Technical Targets

This project is conducting studies of complex hydrides (borohydrides and alanates $LiBH_4$, $Ca(BH_4)_2$, $NaAlH_4$) that are considered to have potential for reversibly storing large amounts of hydrogen. Nanostructured magnesium boride (MgB_2) produced by glancing angle deposition (GLAD) is also being studied for possible enhancement in hydrogenation/dehydrogenation properties. Insights gained from these studies will be applied toward the design and synthesis of hydrogen storage materials. This portion of the project will work towards achieving, among others, the following key DOE 2010 hydrogen storage system targets:

- System Gravimetric Energy Capacity: 2 kWh/kg
- System Volumetric Energy Capacity: 1.5 kWh/L
- System Cost: $4/kWh

Engineered Nanostructures

Accomplishments

- Successfully fabricated magnesium boride nanostructures at room temperature using GLAD.
- System upgrades on our homemade quartz crystal microbalance (QCM) hydrogen storage measurement unit has been done and new measurement procedures has been introduced for accurate hydrogenation/dehydrogenation tests.
- Performed material characterization and preliminary hydrogen storage experiments on GLAD magnesium boride nanostructures.

Introduction

After our previous studies on the model system nanostructured magnesium, we focused our studies on the fabrication and hydrogenation properties of nanostructured magnesium boride during past year. Magnesium borohydride $Mg(BH_4)_2$, which is the fully hydrogenated form of magnesium diboride (MgB_2) was the choice of material due to its promising properties for hydrogen storage applications with a high gravimetric (14.9 wt%) and volumetric density of hydrogen. Many theoretical and empirical studies state the reversibility of $Mg(BH_4)_2$ is possible [1]. The chance of hydrogenating MgB_2 at reasonable pressure and temperatures has been shown in the LiH-MgB_2 systems [2]. The general

approach in the literature has been first starting with the synthesis of magnesium borohydride, dehydrogenate it, and trying to re-hydrogenate it back to magnesium borohydride. However, complete dehydration of $Mg(BH_4)_2$ was not possible at reasonable temperatures, making the following hydrogenation step even more difficult. It has been recently suggested that it may be easier to start hydrogenation process from the fully decomposed magnesium boride (MgB_2) [3]. In addition, due to the reduced size and high surface/volume ratio of nanostructures, it is expected that kinetics of hydrogen adsorption/desorption can be further enhanced for nanostructured magnesium boride.

Approach

The GLAD [4] technique has been utilized for the growth of nanostructured magnesium boride coatings. For GLAD, a sputter/evaporation deposition system with a sample rotation and tilt control capability has been utilized. We used a new QCM gas chamber system that we developed for the hydrogen storage measurements on nanostructured magnesium boride.

Results and Discussion

After various experiments on optimizing the deposition parameters such as sputter power, deposition angle, deposition rate, and initial substrate patterning, the successful method for room temperature fabrication of nanostructured GLAD magnesium was determined to be placing the sample at 90° deposition angle from both sources of magnesium and boron. The sources were located across each other at 180° during the deposition where the sample was rotated around its surface normal axis. At the initial stages of growth, we introduced a formation of a few tens of nanometer long Mg nanoblades by a short Mg-only GLAD thermal deposition. This short pre-deposition was used as a template for the further enhancement of shadowing effect [4] during the following GLAD magnesium boride deposition. Figure 1(a) and (b) shows the top view scanning electron microscope (SEM) images of 270 nm (60 min deposition time) and 540 nm (120 min) thick columnar Mg+B nanostructures obtained from our GLAD experiments. Cross-sectional SEM images (not shown here) also confirm the isolated nanostructure formation. The columnar feature sizes are around 100 nm in diameter for 270 nm long magnesium boride nanostructures and it is about 200 nm for the 540 nm long nanostructures. In addition, Figure 2 shows the X-ray diffraction (XRD) profiles of these Mg+B samples as well as that of uncoated silicon substrate, XRD results indicates that we were able to form a nanostructured MgB_2 coating. However, Figure 2 also shows relatively weak peaks of magnesium, which indicates that the some magnesium atoms couldn't form a boride structure, possibly due to the lack of B or due to the low substrate temperature.

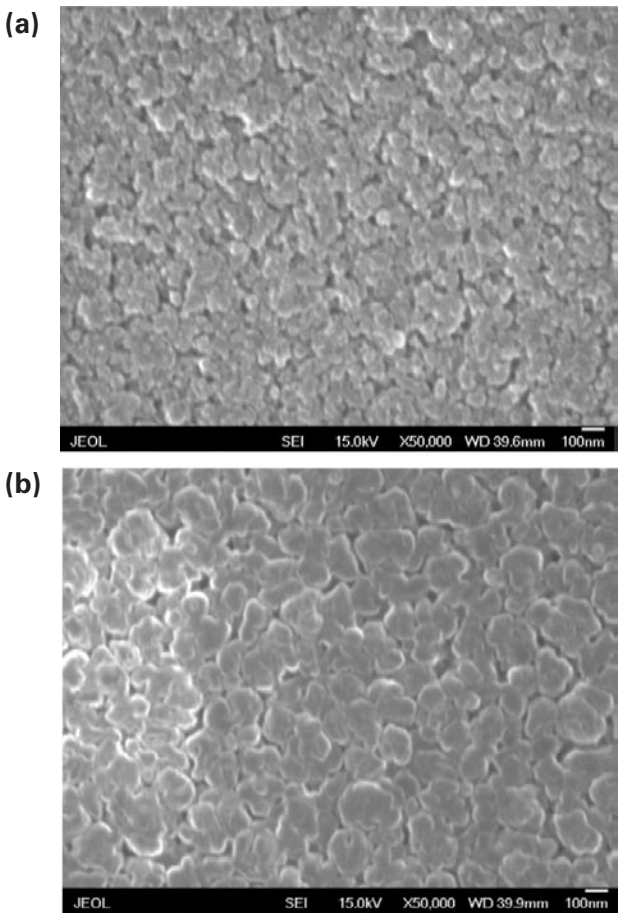

FIGURE 1. Top view SEM images of GLAD nanostructured magnesium boride coatings of thicknesses: **(a)** 270 nm (60 mins deposition time) and **(b)** 540 nm (120 mins) are shown.

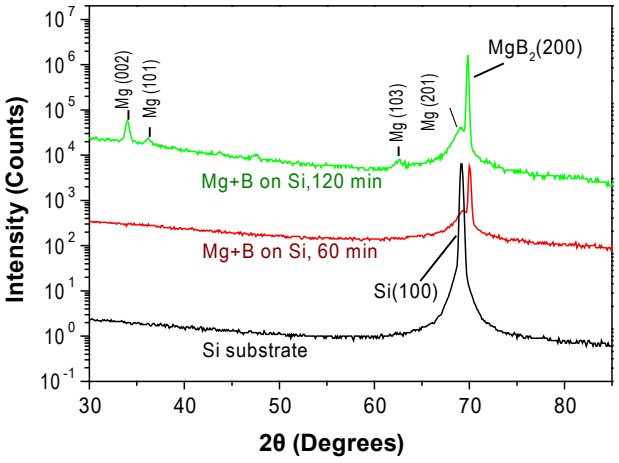

FIGURE 2. XRD profiles of GLAD magnesium boride (Mg+B) samples and uncoated Si substrate are shown. The vertical axis is plotted in log-scale and lines are offset from each other for clarity. Magnesium boride samples have a strong XRD peak at a 2θ angle of about 70.3° that do not belong to neither Mg crystal orientations, or to the silicon substrate. The closest one seems to be that of MgB_2(200), which has a theoretical 2θ value of 70.4°.

In addition, we deposited nanostructured magnesium boride onto QCM crystals in order to analyze its hydrogen absorption propertie using our custom designed QCM chamber. Preleminary QCM results shown in Figure 3 indicate a ~2.9 wt% hydrogen absorption in nanostructured magnesium boride at 300°C under 30 bar hydrogen pressure. The SEM image in Figure 4(a) shows that morphology of the hydrogenated sample is significantly different than the initial product (Figure 3). Columnar features before the hydrogenation process disappeared and a cracked film with finer nano-scale features has formed, possibly due to the coalescence of the magnesium boride nanostructures and crack formation as a result of the volume expansion of the hydrogenated coating. The hydrogenated film did not delaminate from the substrate and was stable after the QCM experiment. XRD analysis on the hydrogenated magnesium boride sample (Figure 4(b)) shows the partial formation of $Mg(BH_4)_2$.

Conclusions and Future Directions

Our results show that we successfully fabricated magnesium diboride (MgB_2) nanostructures at room temperatures using the GLAD method. Preliminary QCM test indicate that we were able to partially hydrogenate MgB_2 at 300°C to form $Mg(BH_4)_2$ with about 2.9 wt% hydrogen storage. However, this storage value is still far below the theoretical maximum value of 14.9 wt%. Therefore we plan to investigate the fabrication of nanostructured magnesium boride with improved crystal and morphological properties and also study the effect of catalyst additives.

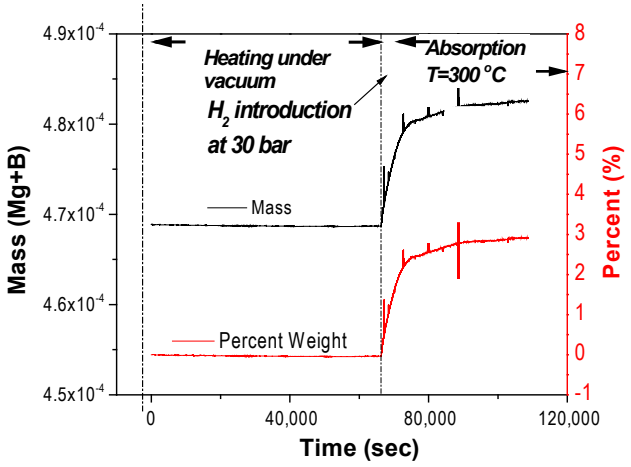

FIGURE 3. Mass (black) and weight percentage change (red) of nanostructured magnesium boride during QCM hydrogen storage experiment is shown. Hydrogen storage value reaches up to about 2.9 wt% under 30 bar H_2 pressure and 300°C chamber temperature.

Plan for Future Studies

Fabrication of nanostructured GLAD MgB_2 at elevated substrate temperatures for enhanced crystallization, with catalyst additives for enhanced hydrogenation/dehydrogenation kinetics, and investigating their hydrogen storage properties.

Borohydrides

Accomplishments

- Examined the catalytic benefits on encapsulation of organic borohydrides in mesoporous silica. Surface chemistry was probed with neutron scattering showing involvement of the surface in decomposition.
- Tested the predicted thermal destabilization effects of the coupled decomposition of $LiBH_4$ and $Ca(BH_4)_2$.
- Performed a thorough investigation of a novel preparations for $Ca(BH_4)_2$ by solid state synthesis.

Introduction

Borohydrides in Mesoporous Silicate

The thermodynamic parameters obtained via ab initio studies predict that many borohydrides are theoretically capable of thermolysis at reasonably low temperatures [5,6]. In practice, much higher temperatures are required, and the rate of reaction is often sluggish except in the presence of a catalyst [7-9]. This implies that the limiting factors are associated with kinetics and the activation energy barrier. Fang et al. have shown that that dispersing $LiBH_4$ with a carbonaceous mesoporous network encourages thermal decomposition [10]. The nature of the interaction between the borohydride and its host network has not been thoroughly investigated as of yet. As a model system, we load organic borohydrides (R_4NBH_4) inside a mesoporous silicate MCM-48. MCM-48 was chosen because it has a regular structure that can easily be probed with XRD, whereas mesoporous carbons derived by templating have irregular pore ordering. Borohydrides with an organic cation provide high visibility of both the cation and anion to neutron scattering and better solvent options for loading the porous networks.

We conducted an additional study on mesoporous silicate loaded with inorganic molecular borohydride $Zr(BH_4)_4$. In addition to thermodynamic benefits, it was anticipated that the silicate will mitigate some of

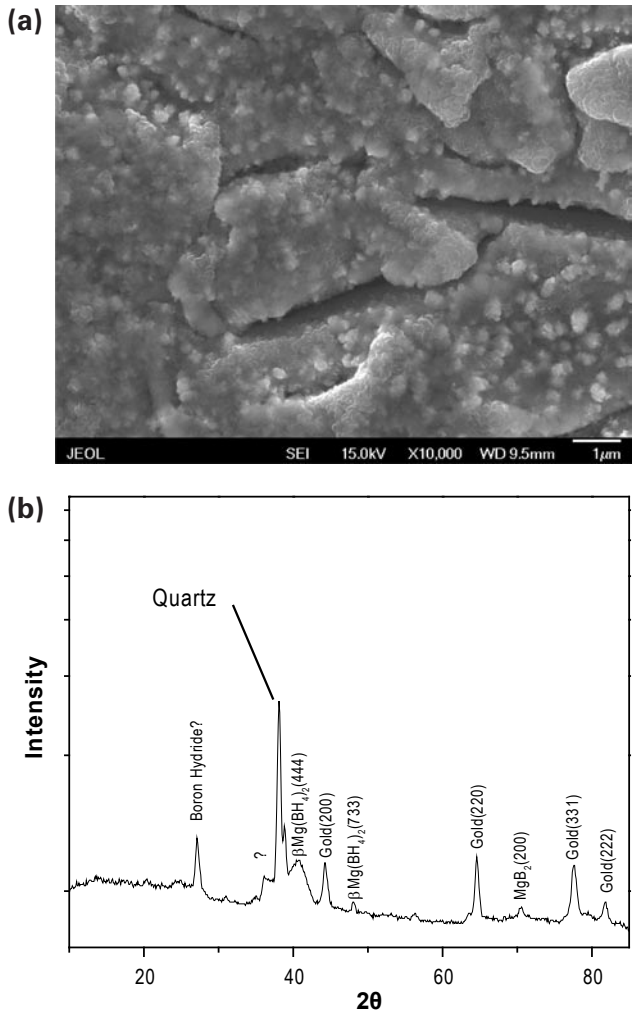

FIGURE 4. Top view SEM image **(a)** and XRD profile **(b)** of nanostructured magnesium boride after QCM hydrogenation experiment at 300°C are shown. XRD results indicate the partial formation of $Mg(BH_4)_2$.

the volatility and reactivity issues with associated with $Zr(BH_4)_4$. The preparation and verification of $Zr(BH_4)_4$ is described in our 1st quarter 2010 report.

Calcium Borohydride Destabilization

$Ca(BH_4)_2$ is a promising candidate for a hydrogen storage material due to its rich hydrogen composition, and lower decomposition ΔH of ~41 kJ mol^{-1} [1]. However, the decomposition of the neat material is sluggish. In practice, the temperatures required to decompose $Ca(BH_4)_2$ are also much higher than the thermodynamics imply [11]. This discrepancy may be due to kinetics. Both of these difficulties may be aided in part by destabilization by coupled decomposition. The following reaction was predicted by Ozolins et al. to have a slightly more attractive enthalpy of ~37 kJ mol^{-1} and comparable hydrogen emission of bulk $Ca(BH_4)_2$ [12].

$$5Ca(BH_4)_2 + 2LiBH_4 \rightarrow Li_2B_{12}H_{12} + 5CaH_2 + 13H_2$$

Additional decomposition with the release of hydrogen is also predicted to be possible from the products by reaction of $Li_2B_{12}H_{12}$ with CaH_2; but the initial step above must occur first. No clear predictions were made regarding the kinetics or reversibility of this reaction, hence our interest in testing it experimentally.

Approach

Borohydrides in Mesoporous Silicate

Mesoporous silicate MCM-48 was synthesized in pressure vessel by hydrothermal methods as described elsewhere [13]. Me_4NBH_4 and Et_4NBH_4 were prepared by wet chemical methods; purity was verified by Fourier transform infrared (FTIR) and XRD. Silicates were loaded with borohydride by incipient wetness methods (see 3rd quarter 2009 report for further preparation details). Loaded compounds were subsequently characterized by differential scanning calorimetry (DSC)/thermal gravimetric analysis (TGA) for thermal analyses, FTIR for general composition and validation, XRD for structural analyses, Brunauer-Emmett-Teller (BET) surface area determination, residual gas analysis to determine the gas product composition and inelastic neutron scattering (INS) to probe the chemical environment inside the pores. INS spectra were collected on the filter difference spectrometer at the Manuel Lujan, Jr. Neutron Scattering Center at Los Alamos National Laboratory.

Calcium Borohydride Destabilization

The theoretically predicted destabilization reaction between $Ca(BH_4)_2$ and $LiBH_4$ was investigated in solid state by ball milling of a stoichiometric mixture of commercially obtained calcium and lithium borohydrides and pressing a pellet of the mixture. DSC/TGA were performed on several pellet samples during heating. Volumetric analyses were also performed on larger samples (~300 mg) of loose ballmilled powder. The sample was heated in a sealed reactor of known volume which was purged by vacuum and backfilled with a small amount of Ar. All preparations were carried out in a helium glove box.

Results and Discussion

Borohydrides in Mesoporous Silicate

The combined results of XRD, FTIR and BET analyses revealed that Me_4NBH_4 and Et_4NBH_4 were

each successfully loaded into mesoporous silicates in uniform fashion (see 3rd quarter 2009 report for further details). TGA analyses revealed that both Me_4NBH_4 and Et_4NBH_4 decompose at lower temperatures when loaded in MCM-48. Figures 5(a) and 5(b) show TGA data for pure R_4NBH_4, and R_4NBH_4 loaded in MCM-48 for R=Me and R=Et respectively. It should be noted that host MCM-48 (not shown) displays no measurable mass loss until temperatures well above 500°C. The thermal analyses in Figures 5(a) and 5(b) reveal that temperature for the onset of decomposition is lowered significantly for both borohydrides when loaded in MCM-48. Mass spectrometry reveals that the primary product of both decomposition reactions is hydrogen. However, the mass spectrum also indicates that a significant quantity of diborane is present in the decomposition gas stream of both R_4NBH_4 compounds. Diborane was present in the bulk decomposition products as well.

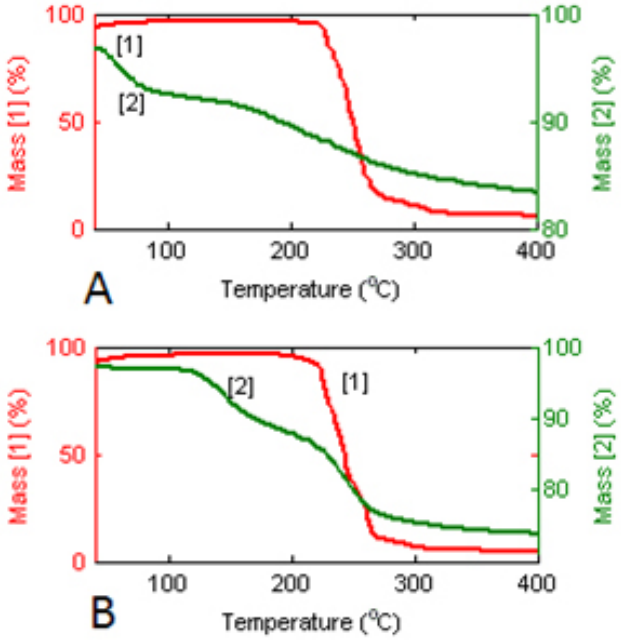

FIGURE 5. **(a)** TGA 5K/min. heating performed under light Ar flow [1]. Bulk Me_4NBH_4 [2]. MCM-48 loaded with Me_4NBH_4, **(b)** TGA 5K/min. heating performed under light Ar flow [1]. Bulk Et_4NBH_4 [2]. MCM-48 loaded with Et_4NBH_4.

INS analyses indicated shifts in frequency and changes in intensity of the vibrational modes of both $[R_4N]^+$ and $[BH_4]^-$ ions after loading in MCM-48. These changes indicate that the ions are adsorbed onto the silica surface, and that the silica surface changes the chemical environment of these borohydrides slightly. Comparisons of the INS spectra of the bulk and loaded compounds of Me_4NBH_4 are shown in Figure 6(a). The spectra of Et_4NBH_4 and its porous silicate loaded counterpart are shown in Figure 6(b). Further evidence of surface interaction is indicated by the formation of surface hydride compounds which occur during vacuum decomposition of Me_4NBH_4. This surface compound was verified to contain a surface Si-H bond by comparison with the INS spectrum of amorphous silica gel with gaseous hydrogen. INS spectra of MCM-48 loaded

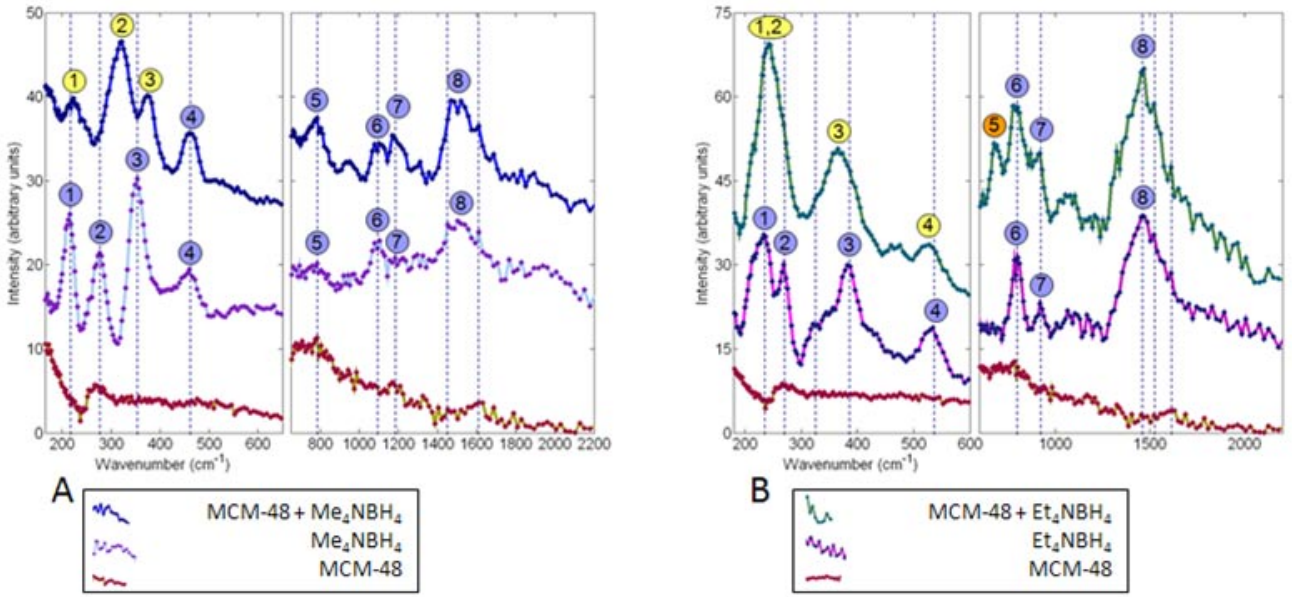

FIGURE 6. **(a)** INS spectra of bulk Me_4NBH_4 and MCM-48 loaded with Me_4NBH_4. Adsorption is apparent from the shifts in frequency of numerous vibrational modes and broadening of spectral features, particularly at low frequencies. **(b)** INS spectra of bulk Et_4NBH_4 and MCM-48 loaded with Et_4NBH_4. Adsorption is apparent from the shifts in frequency of numerous vibrational modes and broadening of spectral features, particularly at low frequencies.

with Me_4NBH_4 after decomposition and the hydrogen exposed silica can be seen in Figure 7(a) and 7(b) respectively. It should be noted that this surface Si-H bond does not form on the decomposition of Et_4NBH_4 adsorbed on MCM-48 nor did it occur in samples of Me_4NBH_4 adsorbed on nickel-doped MCM-48.

$Zr(BH_4)_4$ also adsorbs on MCM-48 with alterations in its chemical environment as observed by INS spectroscopy. Several low frequency normal modes of $Zr(BH_4)_4$ were shifted by significant amounts; with higher frequency modes less affected. Currently $Zr(BH_4)_4$ has been essentially ruled out as a hydrogen storage medium because it becomes volatile upon melting at ~30°C, and decomposes in gas state at ~160°C [14]. This volatility renders the compound unusable in most hydrogen storage systems. TGA data reveal that the $Zr(BH_4)_4$ is retained by the MCM-48 during heating, mitigating the volatility issue. Zirconium was verified to be retained by comparison of the Si:Zr ratio as measured by XRF. The severe sensitivity to moisture of $Zr(BH_4)_4$ in MCM-48 is also apparently reduced somewhat from the bulk compound.

Calcium Borohydride Destabilization

The TGA/DSC curves for the $LiBH_4/Ca(BH_4)_2$ mixture (heated under Ar flow) are shown in Figure 8(a). Two notable endothermic events occur during the heating of the mixture. The endothermic peak at ~115°C coincides with the structural phase transition in $LiBH_4$. The second endothermic peak in the DSC curve of Figure 4b (labeled with a '?') onsets around 200°C. The melting of $LiBH_4$ typically occurs at 285°C, and is greater in total enthalpy change than the structural phase transition at ~120°C and is thus non-consistent with this feature. No melting was evident in the sample upon visual inspection after heating. At higher temperatures, the melting of $LiBH_4$ is notably absent from the DSC curve. There is no such feature in the DSC curve of $Ca(BH_4)_2$, which only begins to decompose at ~350°C [15]. The pressure and temperature data from the volumetric analysis of the $Ca(BH_4)_2/LiBH_4$ mixture is plotted in Figure 8(b). A reaction releasing gas (presumably hydrogen) begins around 220°C. These data are consistent with a thermal destabilization effect from the ballmilling of $Ca(BH_4)_2$ and $LiBH_4$. However, it is unclear if the reaction proceeds as Ozolins et al. [5] predict. FTIR showed the resultant solid residue to be free of the $Li_2B_{12}H_{12}$ product which is the cause of the predicted thermal destabilization (see 4th quarter 2010 report for more details; residual BH_4 was clearly present as well). Also the observed reaction released only 39% of the expected gas emissions that would account for the theoretical reaction of Ozolins et al. This implies partial reaction, or a separate destabilization mechanism.

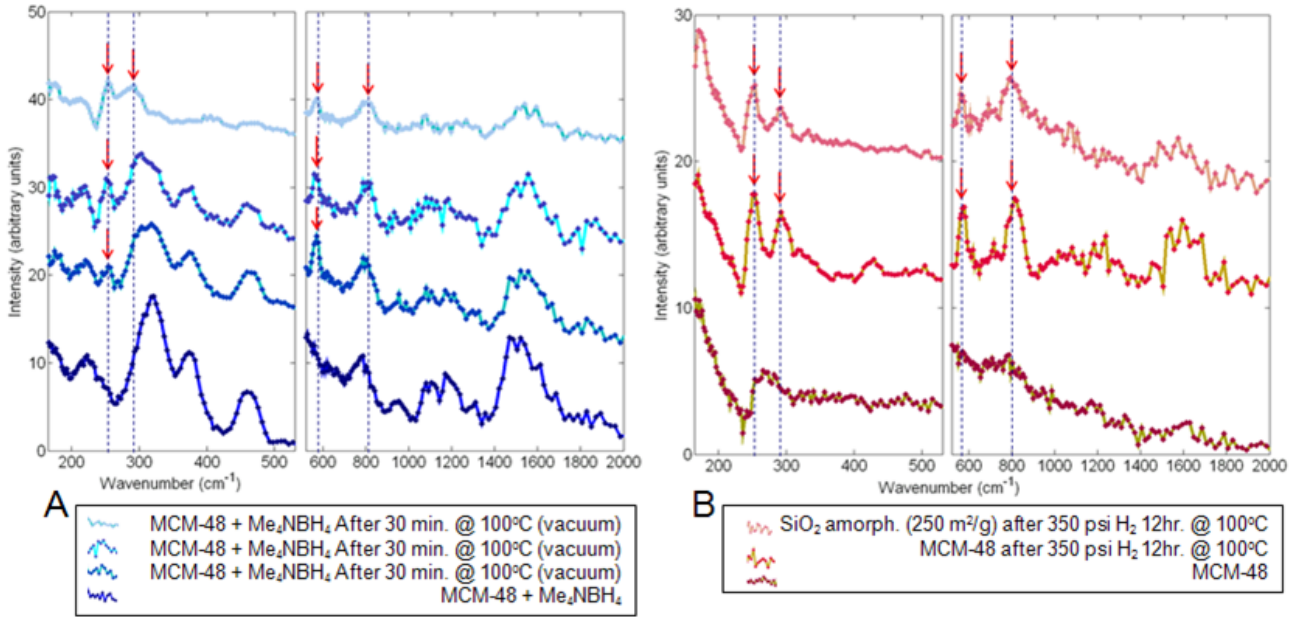

FIGURE 7. **(a)** INS spectra of MCM-48 loaded with Me_4NBH_4 showing thermal decomposition. The sample was decomposed thermally in steps at 100, 200, and 300°C under vacuum. Red arrows indicate features belonging to the surface Si-H compound. **(b)** INS spectra of MCM-48 and high-surface area silica showing the effects of hydrogen exposure (350 psi at 100°C for 12 hr). The maxima of marked peaks occur within less than 5 cm^{-1} of the similarly marked peaks marked in the decomposition of adsorbed Me_4NBH_4.

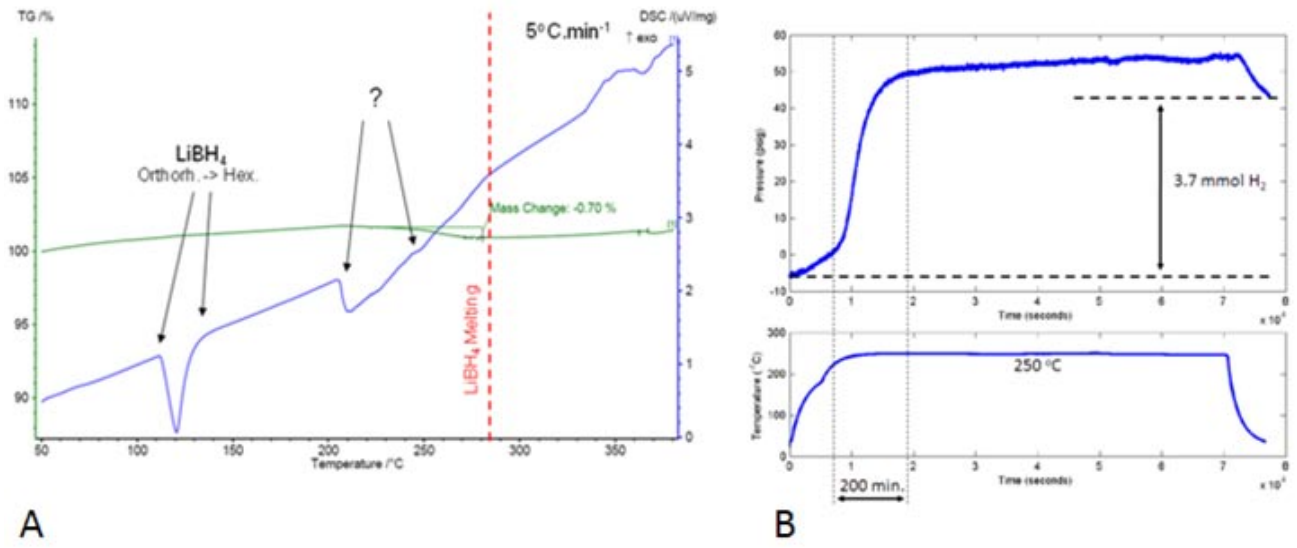

FIGURE 8. **(a)** DSC/TGA of a ballmilled mixture of $LiBH_4$ + $Ca(BH_4)_2$. The second endothermic peak of the DSC indicates a decomposition reaction from destabilization effects. Mass loss is somewhat masked by some trace oxide formation. **(b)** Pressure and temperature readings during heating of a $Ca(BH_4)_2$ + $LiBH_4$ ballmilled mixture sealed in a reactor under light argon backpressure. A reaction releasing 3.7 mmol of gas over 200 minutes occurs at 250°C.

Conclusions and Future Directions

Borohydrides in Mesoporous Silicate

We have demonstrated that adsorption of the borohydrides within the MCM-48 pores provides various utilitarian effects. In Me_4NBH_4 and Et_4NBH_4 a significant reduction (>50°C decrease) in decomposition temperature was observed in TGA for each compound respectively. Rates of thermal decomposition are also improved in the adsorbed compound vs. bulk. Preliminary results indicate that MCM-48 adsorbed $Zr(BH_4)_4$ is retained by the MCM-48 during heating, mitigating the volatility issue. Additionally, the air sensitivity of $Zr(BH_4)4$ is significantly reduced when adsorbed on MCM-48.

Inelastic neutron scattering has revealed that the surface chemically interacts with pore encapsulated borohydrides, and plays some roll in decomposition of adsorbed borohydrides. We have also demonstrated that doping of this network with transition metals can alter the decomposition chemistry.

Calcium Borohydride Destabilization

We have verified a destabilization effect caused by mechanical mixing of $LiBH_4$ and $Ca(BH_4)_2$. The mechanism of this reaction does not appear thus far to be consistent with the theoretically reaction producing $Li_2B_{12}H_{12}$. However, we have not conclusively verified a separate mechanism, and subsequent reaction to decompose the $Li_2B_{12}H_{12}$ may occur. While the observed destabilization is an improvement versus either bulk $Ca(BH_4)_2$ or $LiBH_4$, the reaction temperature, hydrogen yield and kinetics of the observed destabilized decomposition reaction are still require further improvement to be directly usable in hydrogen storage.

Plan for Future Studies

- The effects of surface sites on dehydrogenation of borohydrides may prove useful to future researchers investigating borohydrides for hydrogen storage. The impact on storage capacity and reversibility associated with the use of hydride complexes in porous networks is yet unknown.
- The destabilization of $CaBH_4$ and $LiBH_4$ by solid state mixture has not yet been optimized, and may be viable if it can be further catalyzed by addition of dopants. The products and reversibility are yet unknown.

FY 2010 Publications/Presentations

1. M.F. Cansizoglu and T. Karabacak "Enhanced Hydrogen Storage Properties of Magnesium Nanotrees with Nanoleaves" MRS Fall Conference, 2009, Boston MA.

2. M.F. Cansizoglu and T. Karabacak "Enhanced Hydrogen Storage Properties of Magnesium Nanotrees with Nanoleaves", Mat. Res. Soc. Symp. Proc., Online Paper ID 1216-W05-03.R1 (2010).

3. S.U. Bayca, M.F. Cansizoglu, A. Biris, and T. Karabacak, "Enhanced Oxidation Resistance of Magnesium Nanorods Grown by Glancing Angle Deposition", submitted to Int J Hydrogen Energy.

4. M. Wolverton, L. Daemen, M. Hartl. "Quaternary Ammonium Borohydride Adsorption in Mesoporous Silicate MCM-48" *MRS spring 2010 conference.* San Francisco, CA.

5. M. Wolverton, L. Daemen, M. Hartl. "Quaternary Ammonium Borohydride Adsorption in Mesoporous Silicate MCM-48" *MRS spring 2010 proceedings*. Online paper ID: 1262-W03-03.R1 (2010).

6. M. Wolverton, G. Kannarpady, A. Bhattacharyya "A temperature differential model-based Sieverts apparatus" [submitted].

7. M. Wolverton, G.K. Kannarpady, D. Emanis, A. Bhattacharyya, "Investigation of Titanium Decorated Polyaniline and Polyphyenylacetylene for use as Hydrogen Storage Materials" (in preparation).

References

1. V. Ozolins E.H. Majzoub and C. Wolverton PRL 100, 135501 (2008); H.-W. Li et al. / Acta Materialia 56, 1342 (2008).

2. J.J. Vajo, S.L. Skeith, F. Mertens, Journal of Physical Chemistry B 109, 3719 (2005).

3. G.L. Soloveichik, Y. Gao, J. Rijssenbeek, M. Andrus, S. Kniajanski, R.C. Bowman, Jr., S.-J. Hwang, J.-C. Zhao, International Journal of Hydrogen Energy 34, 916 (2009).

4. T. Karabacak, G.-C. Wang, and T.-M. Lu, J. Vac. Sci. Technol. A 22, 1778 (2004).

5. Ozolins, V.; Majzoub, E.H.; Wolverton, C.J. Am. Chem. Soc. 2009, 131, 230.

6. Siegel, D.; Wolverton, C.; Ozolins, V. Phys. Rev. B. 76, 134102, 2007.

7. Bogdanovic, B.; Felderhoff, M.; Streukens, G.J. Serb. Chem. Soc. 72, 183-196, 2009.

8. Zuttel, A.; Wenger, P.; Rentsch, S.; Sudan, P.; Mauron P.; Emmenegger, C.J. of Power Sources 118, 1-7, 2003.

9. Zaluska, A.; Zaluski, L.; Strom-Olsen, J.O.J. Alloys Compounds, 298, 125, 2000.

10. Fang, Z.; Wang P.; Rufford, T.; Kang, X.; Lu, G.; Cheng, H. Acta Mat. 56, 6257, 2008.

11. Kim, J.H.; Jin, S. A.; Shim, J. H.; Cho, Y.W. Scripta Materialia 2008, 58, 481-483.

12. V. Ozolins, E.H. Majzoub, and C. Wolverton. J. Am. Chem. Soc. 131 (1) p.230-237 (2009).

13. Romero, A.; Alba, M.; Zhou, W.; Klinowski, J.; J. Phys. Chem. B 101, 5294, 1997.

14. Gennari, F; Albanesi, L.; Rios, I. Inorg. Chimica Acta 392 (2009) 3731-3737.

15. E. Ronnebro and E. Majzoub J. Phys Chem. B 111 12045 (2007).